

Electro-optic characteristics and switching principle of a single-cell-gap transfective liquid-crystal display associated with in-plane rotation of liquid crystal driven by a fringe-field

J. H. Song, Y. J. Lim, M.-H. Lee, and S. H. Lee^{a)}

School of Advanced Materials Engineering, Chonbuk National University, Chonju-si, Chonbuk 561-756, Korea

S. T. Shin^{b)}

Department of Display and Semiconductor Physics, Korea University, Chungnam, 339-700 Korea

(Received 10 January 2005; accepted 8 June 2005; published online 30 June 2005)

A single-gap transfective liquid-crystal (LC) display associated with in-plane rotation of the LC director was designed. In the device, a fringe electric field drives to rotate a homogeneously aligned LC in plane to optimize polarization efficiency. Rotating degrees of the LC director, 22.5° and 45° were required in both reflective and transmissive regions, respectively. In the device, the cell gap was the same for both regions, and a dark state was irrespective of the cell retardation value at normal direction, which was highly important in massive fabrications. The switching principle and electro-optic characteristics of the device are reported herein. © 2005 American Institute of Physics. [DOI: 10.1063/1.1991981]

Recently, developments in transfective liquid-crystal displays (LCDs) that show quality visibility under any environmental lighting conditions, while maintaining characteristics such as portability, good legibility, and low power consumption are extensively performed.¹ Recently, many results—such as homogenous cells with a compensation film driven by a vertical electric field (Refs. 2–5) with a dual color filter structure for a dual cell gap, and a single gap transfective display associated with vertical field-driven vertical alignment using multidriving circuit—have been reported.⁶ However, the devices utilizing a vertical electric field exhibit a narrow viewing angle in the transmissive area, since the liquid crystal (LC) director tilts upward or downward in one direction. To overcome a narrow viewing angle, the transfective LCDs using the in-plane switching (IPS) (Refs. 7) and fringe-field switching (FFS) (Refs. 8 and 9) modes which are associated with in-plane rotation of the LC director, is proposed. However, the device using the IPS mode has a design limitation, regarding its ability to determine the ratio of reflective to transmissive areas, and the device using the FFS mode requires a dual cell gap, or a single-cell gap, but dual orientation, which requires an additional process.

In this letter, we propose a single-gap transfective display using the FFS mode with normally black mode, in which the device shows a wide viewing angle in both the reflective (*R*) and transmissive (*T*) areas. Furthermore, the strong merit of the device is a black state, such that the black state of the device in a normal direction is irrespective of the cell retardation value, $d\Delta n$, where d is a cell gap and Δn is the birefringence of the LC.

Figure 1 shows a cell structure of the proposed single gap transfective display. In the device, the array electrodes that have pixel and counterelectrodes exist on the top substrate. The bottom substrate has a patterned reflector and above it, the in-cell retarder with $\lambda/4$ (Ref. 10) exists, which

could, or could not be patterned (here, only nonpattern case is reviewed). One compensation film with $\lambda/4$ exists below bottom substrate. Two polarizers are crossed to each other and an optic axis of the LC coincides with one of the polarizer axes. With this structure, the existence of the in-cell retarder does not increase an operating voltage (V_{op}).

Figure 2 shows an optical configuration of each layer between crossed polarizers. In the *R* area, the polarizer axis and the LC axis coincide with each other, and below the LC layer, the in-cell retarder with $\lambda/4$ making 45° with respect to the polarizer exists, and finally the reflector exists. In the *T* area, the axes of slow axis of the compensation film and the bottom polarizer exist perpendicular to the in-cell retarder and top polarizer, respectively.

Now, let us consider switching a principle of the device, tracing the polarization state on a Poincare sphere, as shown in Fig. 3. Considering the *R* area at first, in the off state, the linearly polarized light (P1) simply passes through the LC layer without a change in the polarization state, and becomes circularly polarized after passing the in-cell retarder (P2). After reflection, the circularly polarized light propagates along a retarder and becomes linearly polarized with a 90° rotation, and then the linearly polarized light just passes the LC layer again, as shown in the Poincare sphere of Fig. 3(a).

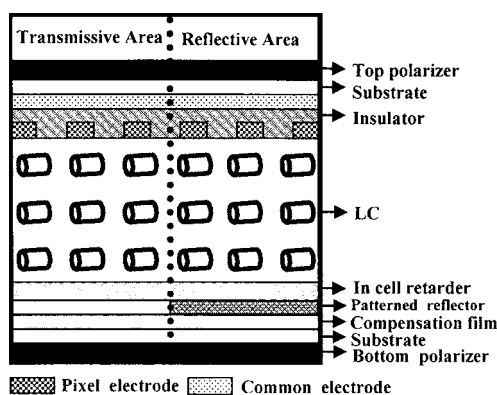


FIG. 1. Schematic cell structures of the fringe-field driven transfective display.

^{a)}Electronic mail: lsh1@chonbuk.ac.kr

^{b)}Electronic mail: stshin@korea.ac.kr

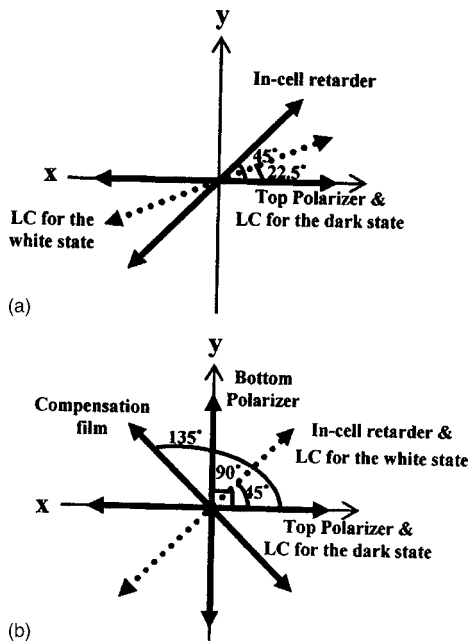


FIG. 2. Optical cell configurations of (a) reflective part and (b) transmissive part.

Then, the cell appears to be black. Now, when the LC director rotates at 22.5° (P3) by the fringe field, the linearly polarized light (P1) only changes direction by 45° (P2), since the effective cell retardation value is assumed to be $\lambda/2$ and it propagates along a slow axis of retarder, without changing polarization state. The reflected light passes the LC cell again and then the vibration direction is the same as the original (P1), resulting in a bright state, as described in Fig. 3(b). Considering the T area, in the off state, the linearly polarized light (P1) passes through the compensation film (P3) such that it becomes circularly polarized. Next, this circularly polarized light passes through the in-cell retarder (P2) whose slow axis is perpendicular to the compensation film, such that it becomes linearly polarized light, returning to an original polarization state. Finally, this light propagates along the LC layer without a change of polarization state, as shown in Fig. 3(c). Thus, it is blocked by the analyzer, which results in a dark state. With the bias voltage, the LC director with an

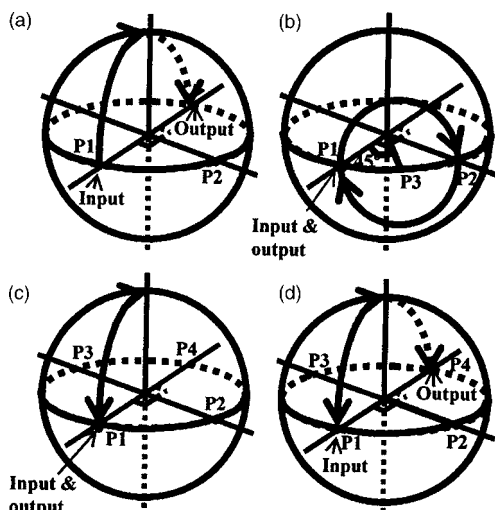


FIG. 3. Poincare sphere representation of the polarization path of the (a) dark and (b) white states in reflective part and the (c) dark and (d) white states in transmissive part.

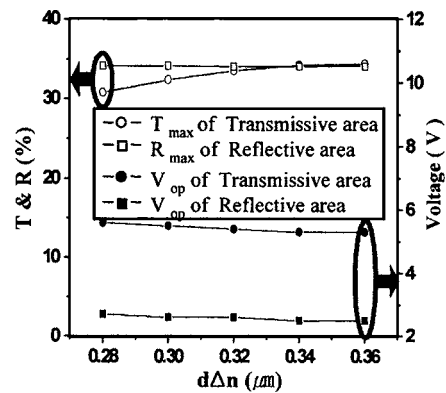


FIG. 4. Maximum reflectance, transmittance, and operation voltages of each area as a function of $d\Delta n$.

effective cell retardation value of $\lambda/2$ rotates at 45° such that the input light (P1) is rotated by 90° (P4) [see Fig. 3(d)], resulting in a bright state.

In order to maximize the reflectance and transmittance, the effective LC cell retardation value should be $\lambda/2$. In the FFS device, the degree of rotation of the LC director is electrode-positional dependent,^{11,12} such that the reflectance and transmittance is dependent on electrode positions. Therefore, the maximal reflectance (R_{max}) and transmittance (T_{max}) on average are calculated as a function of $d\Delta n$, while changing Δn at 550 nm at a fixed cell gap of $4 \mu\text{m}$, as shown in Fig. 4. For the calculations, a LCD master (Shintech, Japan) was used. An electrode structure with an electrode width of $3 \mu\text{m}$ and a distance of $4.5 \mu\text{m}$ between electrodes was considered. Here, the LC with physical parameters, such as dielectric anisotropy $\Delta\epsilon = -4.0$, and elastic constants $K_1 = 13.5 \text{ pN}$, $K_2 = 6.5 \text{ pN}$, $K_3 = 15.1 \text{ pN}$ was used, and the sur-

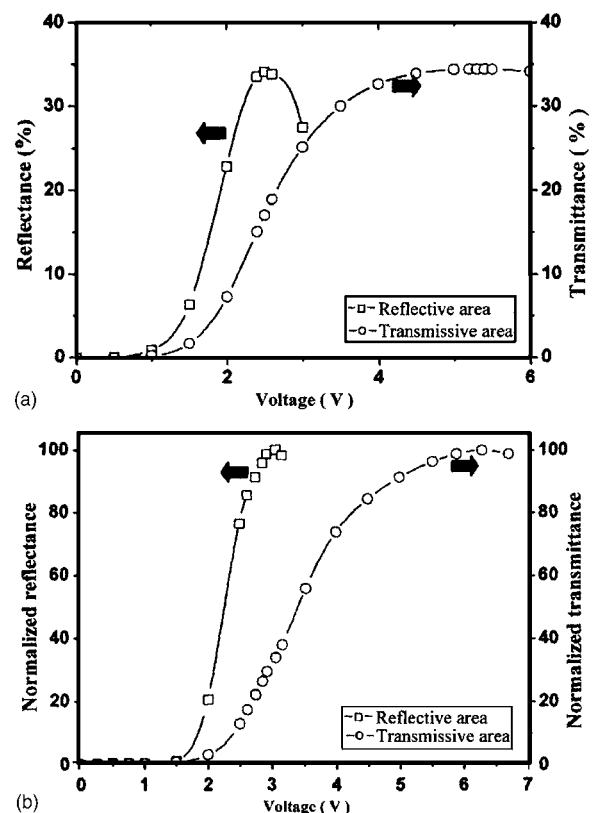


FIG. 5. Calculated (a) and measured (b) voltage dependent reflectance and transmittance curves.

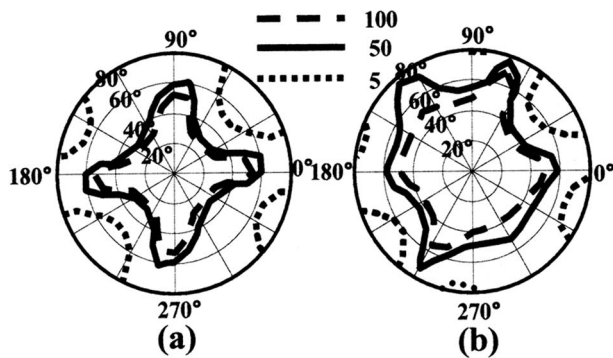


FIG. 6. Calculated isocontrast curves: (a) reflective part and (b) transmissive part.

face tilt angle of the LC was 2° with initial rubbing direction of 12° with respect to horizontal component of a fringe-electric field. Here, to calculate the reflectance and transmittance, a 2×2 extended Jones matrix was used.¹³ The transmittances for the single and parallel polarizers were assumed to be 41%, and 35%, respectively.

As indicated in Fig. 4, the transmittance increases to 35% from 32% as the $d\Delta n$ increases from $0.28 \mu\text{m}$ to $0.36 \mu\text{m}$ but the reflectance is almost the same when the $d\Delta n$ is between $0.28 \mu\text{m}$ and $0.36 \mu\text{m}$. In addition, the $V_{\text{op}s}$ for the *R* and *T* areas slightly decrease to 2.6 V and 5.2 V, respectively, when increasing the $d\Delta n$ up to $0.34 \mu\text{m}$. The difference in the V_{op} between the *T* and *R* areas is due to the difference in the rotating angle of the LC director in the white state. Except for the difference in the V_{op} , the device has a relatively wide margin in cell retardation value because the white state and the V_{op} do not change rapidly as the $d\Delta n$ changes. Additionally, the dark state of the device at normal direction is insensitive to the $d\Delta n$ variation, which is highly required in real cell fabrication for mass production. Considering maximization of the light efficiency and low V_{op} , we have chosen the cell retardation value to be $0.36 \mu\text{m}$. With these cell parameters chosen, we calculated a voltage dependent reflectance and transmittance, as shown in Fig. 5(a). Unfortunately, two curves do not coincide with each other, which requires further optimization for both curves to match one another to use a single driving circuit. A test cell was fabricated and evaluated to confirm the feasibility. Here, the electrodes and other cell conditions were the same as those in calculation, and the thickness of the in-cell retarder was $1 \mu\text{m}$. The voltage dependent reflectance and transmittance was measured, as shown in Fig. 5(b). The V_{op} in the *R* area was one-half (3.1 V) of that (6.3 V) in the *T* area, which correlated with the calculated results. Finally, the viewing angle characteristics were calculated at 550 nm, as shown in Fig. 6. The uniformity of the white state in both the reflectance and transmittance was excellent, and also remarkably the dark state was obtained. Consequently, in the *R* area, the

region in which the contrast ratio (CR) was larger than 5 exists to about 50° of polar angle in all directions, except in certain diagonal directions, where it exists larger than 80° of polar angle. In the *T* area, the region in which the CR was larger than 10 exists over 60° of polar angle in all directions. Furthermore, the device does not show grey scale inversion at any of the given viewing angle range, since the LC director rotates almost in plane.

In summary, we have proposed a single-gap transfective display, in which the homogeneously aligned LC director rotates almost in plane, driven by a fringe-electric field. In the device, the LC director rotates at 22.5° and 45° in the reflective and transmissive areas, respectively, such that the operation voltage in the reflective area is one-half of that in the transmissive area. Further, with an array of electrodes on the top substrate and an in-cell retarder below the LC layer, a relatively low operating voltage can be achieved. Owing to the in-plane orientation of the LC director, the device exhibits an excellent viewing angle without the occurrence of grey scale inversion in a polar angle of 50° , in all directions, in both the reflective and transmissive areas, such that the device overcomes the long-standing problem of the conventional vertical-field driven transfective displays. We expect that this concept of device accelerates the application of a wide viewing angle in a single-gap transfective LCDs.

This work was supported by Grant No. R01-2004-000-10014-0 from the Basic Research program of the Korea Science and Engineering Foundation.

¹R. Watanabe and O. Tomita, *Proceedings of the Ninth International Display Workshops*, 2002, p. 397.

²T. Uesaka, E. Yoda, T. Ogasawara, and T. Toyooka, *Proceedings of the Ninth International Display Workshops*, 2002, p. 417.

³K. Fujimori, Y. Narutaki, Y. Itoh, N. Kimura, S. Mizushima, Y. Ishii, and M. Hijikigawa, *Dig. Tech. Pap. Society for Information Display Int. Symp.*, 2002, p. 1382.

⁴Y. Narutaki, K. Fujimori, Y. Itoh, T. Shinomiya, N. Kimura, S. Mizushima, and M. Hijikigawa, *Proceedings of the Ninth International Display Workshops*, 2002, p. 299.

⁵K.-J. Kim, J. S. Lim, T. Y. Jung, C. Nam, and B. C. Ahn, *Proceedings of the Ninth International Display Workshops*, 2002, p. 433.

⁶S.-G. Kang, S.-H. Kim, S.-C. Song, W.-S. Park, C. Yi, C.-W. Kim, and K.-H. Chung, *Dig. Tech. Pap. Society for Information Display Int. Symp.*, 2004, p. 31.

⁷J. H. Song and S. H. Lee, *Jpn. J. Appl. Phys., Part 2* **43**, L1130 (2004).

⁸T. B. Jung, J. H. Song, D.-S. Seo, and S. H. Lee, *Jpn. J. Appl. Phys., Part 2* **43**, L1211 (2004).

⁹Y. J. Lim, J. H. Song, and S. H. Lee, *Jpn. J. Appl. Phys., Part 2* **43**, L972 (2004).

¹⁰S. J. Roosendaal, B. M. I. van der Zander, A. C. Nieuwkerk, C. A. Renders, J. T. M. Osenga, C. Doornkamp, E. Peeters, J. Bruinink, and J. A. M. M. van Haaren, *Dig. Tech. Pap. Society for Information Display Int. Symp.*, 2002, p. 78.

¹¹S. H. Lee, S. L. Lee, and H. Y. Kim, *Appl. Phys. Lett.* **57**, 2881 (1998).

¹²S. H. Jung, H. Y. Kim, M. H. Lee, J. M. Rhee, and S. H. Lee, *Liq. Cryst.* **32**, 267 (2005).

¹³A. Lien, *Appl. Phys. Lett.* **57**, 2767 (1990).